JOURNAL OF SOLID STATE CHEMISTRY 37, 112–121 (1981)

Elastic Strain Energy and Microstructures of Orthorhombic Tin–Tungsten Bronzes

E. IGUCHI* AND R. J. D. TILLEY†

Department of Metallurgical Engineering, Faculty of Engineering, Yokohama National University, Tokiwadai, Hodogaya-ku, 240 Japan, and †School of Materials Science, University of Bradford, Bradford, W Yorks BD7 1DP, United Kingdom

Received April 28, 1980; in final form July 24, 1980

The elastic strain energy of the series of orthorhombic I bronzes which occur in the Sn–W–O system has been calculated using the Fourier transform method. The results of these calculations are compared with microstructures and phase analysis carried out by transmission electron microscopy. The two are in good agreement, suggesting that elastic strain energy is important in materials containing planar faults other than crystallographic shear phases.

Introduction

When WO_3 is reacted with small amounts of metals or metal oxides the change in stoichiometry is sometimes accommodated by the formation of planar defects in the WO_3 structure. Thus when WO_3 reacts with Nb_2O_5 or Ta_2O_5, crystallographic shear (*CS*) planes are formed, which, when ordered, result in homologous series of *CS* phases (*1*). Anderson suggested that elastic strain energy could well play a significant role in controlling the microstructures of these *CS* phases (*2*) as the *CS* planes themselves could be regarded as defects within an otherwise ordered crystal. Following this suggestion Iguchi and Tilley calculated the strain energy due to *CS* planes in WO_3 and quantitatively explained the microstructures observed in nonstoichiometric WO_3 rather well by considering that they were produced as a result of attempts to minimize the elastic strain energy (*3–6*). Similarly Shimizu and Iguchi succeeded in analysing *CS* plane behavior in rutile (TiO_2) again by using strain energy calculations (*7*).

Because of this success it seemed natural to attempt the same sort of calculation for at least one type of material which is not a *CS* phase. A suitable series of structures are to be found in the Sn_xWO_3 system. At low tin concentrations a series of orthorhombic bronze phases form, which have structures which may be likened to WO_3 containing planar faults (*8*). Although the structures are not known in detail, they are sufficiently resolved for our purposes and recent careful phase analysis studies on these materials (*9*) has given us sufficient data to compare with elastic strain energy calculations.

In this report we present the results of these elastic strain energy calculations and compare them to new and existing data.

0022-4596/81/040112-10$02.00/0

Sample Preparation and Characterization

Samples with an overall composition between $Sn_{0.01}WO_3$ and $Sn_{0.10}WO_3$ were prepared by heating tungsten trioxide with tin metal in evacuated silica ampoules. The tungsten trioxide was in the form of a fine powder and the tin in the form of turnings from a metal rod. All chemicals were of Specpure grade and supplied by Johnson Matthey Ltd. A heating time of 20 days at 900°C was employed, after which the ampoules were quenched into water.

After reaction the materials present in the tubes were examined in a JEM 100B electron microscope fitted with a goniometer stage, as described previously (*9*). The crystal types were analyzed by consideration of their microstructures as revealed in electron micrographs and their diffraction patterns. Typical examples are illustrated in Fig. 1, and fuller details will be found elsewhere (*9*). The number of crystal fragments examined for each sample prepared was more than 20, and the results of this examination for compositions falling within the phase range of interest are listed in Table I. In this report we will consider only those phases which fall into the group which we have designated as orthorhombic I bronzes. In Table I this corresponds to those crystals in which n varies from 7 to 14 inclusive, as the bronzes with $n = 5$ or 6 can also have somewhat different structures (*8*, *9*).

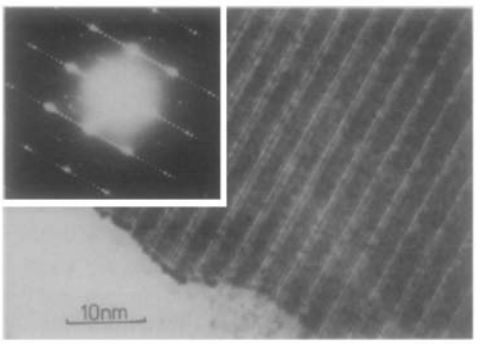

FIG. 1. An electron micrograph of a typical Sn_xWO_3 orthorhombic I bronze crystal showing slabs of WO_3-like structure united along planes in which the exact structure is unclear. The diffraction pattern of the phase is inset and shows an intense spot approximately every 9 subcell reflections, revealing that the crystal is a "9-type" bronze fragment.

TABLE I

ELECTRON MICROSCOPE ANALYSIS OF CRYSTAL FRAGMENTS FROM Sn_xWO_3 PREPARATIONS SPANNING THE COMPOSITION RANGE FROM $Sn_{0.01}WO_3$ TO $Sn_{0.10}WO_3$[a]

x in Sn_xWO_3	Total number of fragments	Orthorhombic I Bronzes, n value										
		Disordered	14	13	12	11	10	9	8	7	6	5
0.02	23	4		1	6	5	1	1	4	1		
0.03	29[b]	5	1	1	4		1	1	8	7		
0.04	23	5			3	1	8	3	3			
0.05	24									16	8	
0.06	24									4	19	1
0.07	22									6	14	2
0.08	22									2	20	
0.09	23									1	20	2
Total		14	1	2	13	6	10	5	15	37		

[a] The fragments corresponding to $n = 6$ and 5 can exist in a different structure to the phases considered here and do not figure directly in the analysis.

[b] One fragment contained {102} *CS* planes only.

The crystal structures of these materials are not known with certainty. The micrograph shown in Fig. 1 reveals that the structures are composed of WO_3-like slabs of material separated by ill-defined planar boundaries. The structural work which has been done (*8*) suggests the model shown in Fig. 2 for these faults. The defects consist of planes of tin ions and as can be seen in Fig. 2, each planar defect in an n-type structure is bridged to neighboring faults on either side with arrays of $(n - 1)$ WO_6 octahedra. The spacing between the nearest neighboring oxygen ions in the fault plane reduces to approximately (4/5) of the spacing of oxygen ions in the idealized WO_6 octahedra for the 7- and 8-type structures so far investigated. In the matrix between the two fault planes, the tungsten ions deviate a little above or below the mirror plane alternately as shown in Fig. 2.

Strain Energy due to Planar Defects

In order to discuss the experimental results quantitatively in terms of the strain energy, the forces acting in the defect planes must be estimated. As the orthorhombic-I tin–tungsten bronzes possess planar defects similar to *CS* planes, we can suppose that the defect forces in these planar defects are similar to those originating in *CS* planes in WO_3 (*3–6*) and in TiO_2 (*7*). In this report, therefore, we have calculated the strain energy due to an infinite ordered array of n-type planar defects (n = 5–15) in a tin–tungsten bronze crystal in a similar way to the calculations made for *CS* planes in rutile (*7*), and WO_3 (*5, 6*) using the so-called Fourier transform method, the details of which are set out in the Appendix.

In order to simplify the calculation as much as possible, we have employed the idealized structures shown in Fig. 3 in which every tungsten ion is in the mirror plane instead displaced as in the real structures shown in Fig. 2 and we have also assumed that the crystal structure of the WO_3-like part of the structure is of the idealized cubic ReO_3 (DO_9) type as in our previous papers (*3–6*). According to the data given above (*8*), the spacing between the nearest neighboring oxygen ions in the defect planes is assessed to be approximately $4(2)^{1/2}a/10$ which is about 4/5 of the spacing between oxygen ions in the idealized WO_6 octahedron. We have assumed that this will be so for all members of the bronze series and so have taken the spacing between oxygen ions in the planar defects concerned in this paper to be

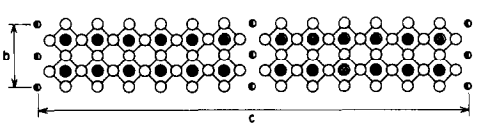

FIG. 2. Projection of the proposed structure of an n = 7 bronze along [010]. The small filled circles are octahedrally coordinated tungstens which are a fraction (x = 0.07) above the mirror plane. The small circles containing a cross are tungstens at the same distance below the mirror plane. The half-filled circles represent tin atoms.

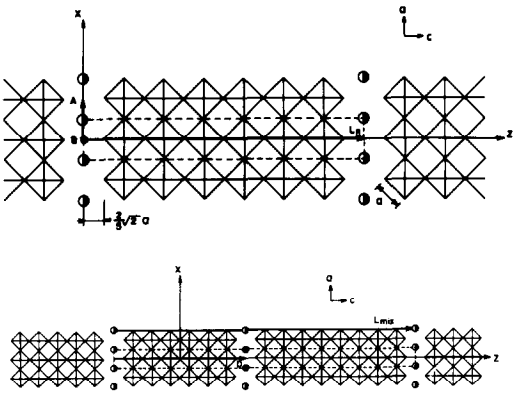

FIG. 3. (a) The idealized structure of the n = 7 bronze. The broken line represents the periodic unit cell. The vectors **A**, $\mathbf{L}_n$ are in {010} and **B** is normal to {010}. The coordinate axes are also shown and a is the octahedron edge. (b) The idealized structure in an ordered crystal $(n + 1)$, $(n - 1)$ in which n = 8. The origin of the coordinates in the "two phase mixture" is taken to be midway along the vector **D** from the origin in the unit of the 7-type to that of the 9-type.

$4(2)^{1/2}a/10$ regardless of the n value of the bronze concerned.

The periodic unit cell for an infinite ordered array of planar defects can be constructed with the vectors, **A**, **B**, and $\mathbf{L}_n$; the projection of the unit cell in the {101} plane being outlined by the broken line in Fig. 3. We have arbitrarily chosen the origin of the coordinates to be between tin ions in a tin-plane, and taken the x, y, and z axes to be parallel to the unit cell edges, as indicated in Fig. 3. The vectors, **A**, **B** and $\mathbf{L}_n$, are expressed in terms of the primitive translation vectors of the WO_3 lattice, **a**, **b**, and **c** as follows:

$$\begin{aligned} \mathbf{A} &= 2\mathbf{a} \\ \mathbf{B} &= 2\mathbf{b} \\ \mathbf{L}_n &= 2(5n-1)\mathbf{c} \\ \mathbf{a} &= (a/2)\mathbf{i} \\ \mathbf{b} &= (a/2)\mathbf{j} \\ \mathbf{c} &= (a/10)\mathbf{k} \end{aligned} \tag{1}$$

where the vectors, **i**, **j**, and **k**, indicate the unit vectors along the x, y, and z axis, respectively, and a is the length of an octahedron edge. The structure of an infinite ordered array of planar defects can then be constructed by the formal geometrical translation vector **T** which can be expressed by linear combinations of **A**, **B**, and $\mathbf{L}_n$ thus,

$$\mathbf{T} = n_1\mathbf{A} + n_2\mathbf{B} + n_3\mathbf{L}_n \tag{2}$$

where n_1, n_2, and n_3 are integers.

If we assume an ionic structure for the planar defects, the major forces will be ones of repulsion between the nearest neighboring oxygen ions. On the other hand, the interactions between tin ions and oxygen ions in the plane are expected to be ones of attraction. Therefore, we have suggested the defect forces as shown in Fig. 4 to be those of importance and consider them to be composed of the summation of the repulsive forces between oxygen ions and the attractive forces between tin ions and oxygen ions. These forces, which are essentially due to chemical bonding, can be taken as short-range interactions.

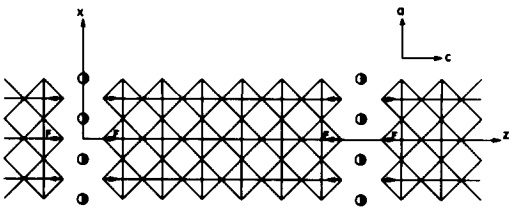

FIG. 4. The defect forces suggested for a 7-type orthorhombic bronze.

For completeness we should also consider possible long-range interactions. However, we should note that long-range forces can be screened fairly readily and are not easy to treat theoretically. For example, both point defects or altered charge states of ions can screen electrostatic and other long-range electronic interactions. The addition of altervalent ions as impurities can also have significant effects here. Ions with considerably different sizes to tin or tungsten will substantially influence elastic strain fields and other related long-range forces. Thus, to estimate these long-range interactions in any detail the physical properties of WO_3 must be known. Unfortunately those of relevance have not yet been reported, but taking into account the crystallographic symmetry of the planar defects the forces due to the long-range interactions may be reasonably supposed to act normal to the planar fault. We therefore assume that the defect force F shown in Fig. 4 may be taken to represent the summation of the forces due to the short-range and the long-range interactions.

At present, we have no information as to whether F is positive or negative, but this does not matter at all because the strain energy equations contain only F^2 terms. Also we cannot assess the value of the defect forces, but we can calculate the relative values of the strain energy due to

each orthorhombic bronze in this report, if we assume that the value of the forces does not depend on the width of the WO_3-like slabs separating the tin planes.

Indeed, we can take this argument a little further. It is clear from the electron micrograph shown in Fig. 1 that the faults lie along {001} planes referred to an idealized WO_3-like matrix, and it seems consistent to assume that the net defect force, F, will be normal to this fault plane regardless of the precise structure of the fault plane itself. For example, we have made a number of possible models for these and similar fault planes in Pb_xWO_3 (*11*) as well as Sn_xWO_3 (*9*). If one suggests ionic interactions of the sort described above for any of these alternative structures the most likely net force is normal to the fault plane. Despite some uncertainties in the initial structures chosen, we are therefore confident that the results of the calculations will be valid for these structures even if changes in the fault plane structure are envisaged.

The compactness of the Fourier transform method of calculation also allows us to treat other geometries besides the ordered array of evenly spaced fault planes, separated by n WO_3-like octahedra, just described. One of the simplest is to consider the geometry n_1, n_2, n_1, n_2 and we have also calculated the elastic strain energy for two of the most relevant of these situations. The first arrangement we have considered is represented in Fig. 3b where we show the couple $n_1 = n - 1$ and $n_2 = n + 1$. The theoretical treatment is the same as for an infinite ordered array except for the following points. As shown in Fig. 3b, we have chosen the origin of the coordinates in the "two phase" mixture to be midway along the vector **D**, from the origin of the unit cell of the (n-type) region to that of ($n + 1$) region. Then, the vector **D** is written as

$$\mathbf{D} = 2(5n - 6)\mathbf{c}. \tag{3}$$

The Fourier-transformed force of the "two phase" mixture, $\tilde{F}_{\text{mix}}(\mathbf{q})$ can be obtained in a similar way to the calculation for a pair of *CS* planes by Stoneham *et al.* (*15*), i.e., the vector $\mathbf{L}_n$ in Eq. (2) is, then, replaced by the vector $\mathbf{L}_{\text{mix}}$ shown as follows

$$L_{\text{mix}} = \mathbf{L}_{n-1} + \mathbf{L}_{n+1} = 2\mathbf{L}_n. \tag{4}$$

The second geometry considered is represented by the couple $n_1 = n$, $n_2 = n + 1$. In this case, the theoretical treatment is the same as that in the case of the couple $n_1 = n - 1$ and $n_2 = n + 1$ except for the following points,

$$\mathbf{D} = 2(5n - 1)\mathbf{c}$$

$$\mathbf{L}_{\text{mix}} = \mathbf{L}_n + \mathbf{L}_{n+1}. \tag{5}$$

Results and Discussion

Using the relations described above and in the Appendix we have calculated the strain energy due to an infinite ordered array of planar defects for a number of interplanar spacings. The strain energy per unit volume of these crystals as a function of the n-value is shown in Fig. 5. In this figure the vertical axis is in units of $[(F/\pi)^2/C_{44}]/[L]^3$, so that the strain energy per unit volume can be obtained by dividing

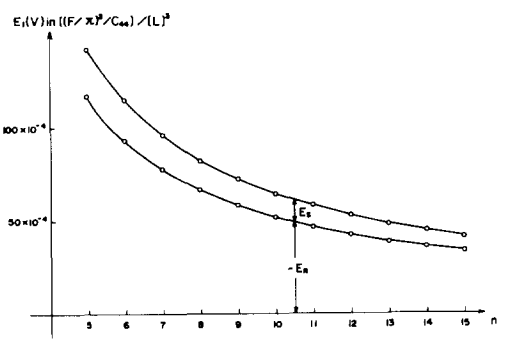

FIG. 5. The strain energy per unit volume plotted as a function of n. The strain energy is represented in units of $[(F/\pi)^2/C_{44}]/[L]^3$. The strain energy is the summation relaxation energy, $-E_R$, and the strain energy of ions, E_S, which are also indicated.

$[(F/\pi)^2/C_{44}]/[L]^3$ by the lattice constant a, where $|L|$ possesses the dimension of length. If C_{44}, F, and a are represented in units of J nm^{-5}, J nm^{-3}, and nm, respectively, $|L|^3$ will be nm^3. The strain energy is the summation of the relaxation energy ($-E_R$) and the strain energy of ions (E_S), which are also indicated in Fig. 5. The relaxation energy is always negative, which coincides with the results for *CS* planes in rutile (*7*) and WO_3 (*5, 6*).

This result shows that the strain energy increases smoothly as we decrease the n-value of the phases. This is quite reasonable because as the n-value decreases, the density of the planar defects increases and the strain energy per unit volume increases. This is in agreement with the results found for rutile or WO_3 which have ordered arrays of *CS* planes. One of the more interesting features of these calculations is the magnitude of the relaxation energy. Figure 5 shows that the relaxation energy plays a major role in the overall strain energy and because it is negative in sign it is also seen that it is important in stabilizing the planar faults. We will return to this aspect later in this section.

Previous calculations for *CS* phases (*3–6*) suggest that the elastic strain energy of each member of the series may contribute significantly to its stability and hence to the probability of preparing the phase experimentally. It is reasonable to assume for example, that if a homolog n decomposes into its neighbors, homologs $n + 1$ and $n - 1$, and the total elastic strain energy of the system falls, such a decomposition will take place in practice. Hence the $n - 1$ and $n + 1$ phases will accumulate in preparations at the expense of the n homolog, which may not, in fact, actually form.

We can estimate the stability of each of the compounds considered, relative to a disproportionation of the sort described in the following way. The energy per unit volume of the "two phase" mixture of $(n + 1)$, $(n - 1)$ faults is denoted as E_{mix}. The difference in energy per unit volume, $\Delta E = E_n - E_{mix}$, is shown in Fig. 6 as a function of n. The ordered n array will be stable if ΔE is negative, while if ΔE_n is positive, it will be less stable than the $(n + 1)$ and $(n - 1)$ neighbors on either side of it and so, if possible, will disproportionate to these phases. The result in Fig. 6 shows that ordered arrays with values of n less than 10 and also $n = 12$ are stable while the phases with $n = 11$ and 13, 15 are unstable.

It is of some interest to compare this result with the experimental findings. It is clear from Fig. 6 that once we progress beyond n values of about 13 the phases are unstable with respect to disproportionation. This will lead to a phase separation into $n = 12$ and, because of continued disproportionation, some very much higher stable homolog, or else WO_3. Indeed as no appreciably higher n values than 12 have been found abundantly, it would seem likely that $n = 12$ is the highest of the stable phases from a point of view of elastic strain energy. At lower degrees of reduction we find that all phases are stable, with respect to this disproportionation, in good accord with the experimental results.

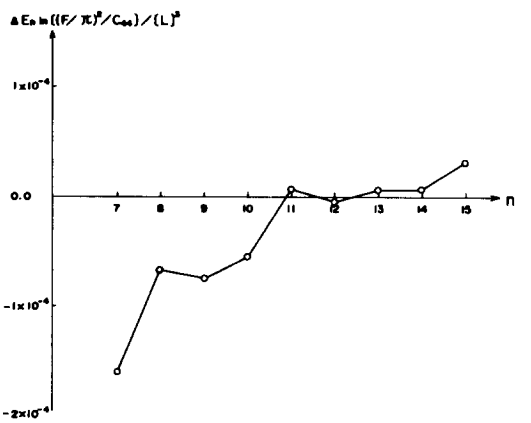

FIG. 6. ΔE, the difference between E_n and E_{mix} as a function of n. The units on the vertical axis are the same as in Fig. 5.

In previous phase analyses in this system (*9*) we have occasionally observed crystals which are composed of ordered arrays n, $n + 1$ rather than just n. It is also worth while, therefore, to compare the elastic strain energy of these two situations. The elastic strain energy of the n, $n + 1$ array is shown in Fig. 7a. If the values are compared with those in Fig. 5 it is seen that they are very similar indeed. This indicates that there is little difference in elastic strain energy between an n or $n + 1$ array and an ordered n, $n + 1$ array.

In order to take this further we need to compare the values in Fig. 5 with those in Fig. 7a more closely. It is impossible, in the strict sense, to compare the stability of an ordered n, $n + 1$ series and an ordered n array because

$$L_{max} = L_n + L_{n+1} \neq 2L_n.$$

However, if we imagine an ideal crystal which consists of two regions, one containing an ordered n array, the other an ordered $n + 1$ array and the interaction between these regions is assumed to be the same as that between planar defects in the ordered n or $n + 1$ array, the strain energy in such a crystal can be expressed as $(E_n + E_{n+1})/2$ where E_n represents the strain energy per unit volume of the crystal containing the ordered n array. Then we might compare the strain energy of the n, $n + 1$ ordered array per unit volume, $E_{n,n+1}$, with $(E_n + E_{n+1})/2$. This result is shown in Fig. 7b where the vertical axis represents $(E_n + E_{n+1})/2 - E_{n,(n+1)}$ and the horizontal axis represents the couple n, $n + 1$ or $[n + (n + 1)]/2$. It is apparent that the ordered n, $n + 1$ array has a slightly higher elastic strain energy than the equivalent ordered n arrays. Thus if the assumptions described above are appropriate, the ordered n, $n + 1$ array would always appear to be unstable in comparison with the ordered n arrays.

This result is in good agreement with the

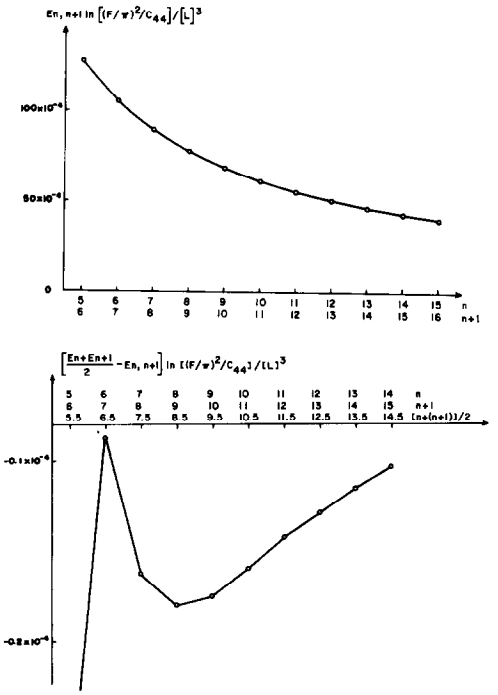

FIG. 7. (a) The strain energy per unit volume of an n, $n + 1$ mixed array as a function of n, $n + 1$. (b) The difference between $\frac{1}{2}(E_n + E_{n+1})$ and $E_{n,n+1}$ as a function of n, $n + 1$ or $[n + (n + 1)]/2$.

fact that ordered n, $n + 1$ arrays are rarely found, compared with ordered n arrays. However the elastic strain energy difference is so small that should an n, $n + 1$ array form it would seem unlikely that elastic strain energy would provide sufficient driving force to unmix the array into two separate regions. A mechanism for the formation of these phases in a mechanical fashion has been put forward earlier (*11*) and the present results tend to support such a mechanical model for the formation of these arrays, and that, once formed, there is little to be gained energetically from unmixing into separate phases.

We finally return to the question of relaxation energy. It has already been pointed out that the relaxation energy in these phases is high, and we can note that a high relaxation energy would seem to be impor-

tant in the balance of factors which decide whether a nonstoichiometric system will adopt point defects or planar faults to accommodate changes in anion to cation ratio. The first indirect suggestion to this effect was when it was appreciated that planar faults seem to be preferred in materials which showed a high static dielectric constant (*16, 17*). It is well known that high degrees of ionic or atomic relaxation will indeed result in a high macroscopic dielectric constant.

This was taken further by Catlow and James (*18, 19*) who have calculated the formation energy of *CS* planes in Ti_5O_9 and find that the considerable degree of relaxation of the ions within the *CS* plane appears to be the factor which determines that planar faults are to be preferred to point defects in this system. It is clear, therefore, that the relaxation of the tin atoms in the planar faults contributes substantially to the stability of the planar fault geometry found here. In this context it is easy to appreciate that the relaxation of tin atoms in a planar fault could be significantly greater than in the octahedral environment that would hold if tin substituted for tungsten in WO_3, as SnO_2 itself, in which tin is octahedrally coordinated, has a low dielectric constant. It is, though, difficult to understand why the planar fault geometry would give a greater degree of relaxation than, for example, tin interpolated into the cages in the WO_3 structure to form a perovskite related bronze structure with a formula Sn_xWO_3. Further experiments are underway to try to clarify some of this obscurity, both in the Sn–W–O system and in other related ternary tungsten oxides.

We can finally note that very closely related structures to those illustrated here for these tin tungsten oxides occur in a number of perovskite related oxides, notably of titanium and niobium. (see *20, 21* and the references therein.) It is possible that the stabilities of these phases may depend critically upon elastic strain energy, and the extent of the composition ranges over which ordered phases extend may be influenced by whether disproportionation to neighboring structures increases or decreases the elastic strain energy of the system as a whole. Elastic strain energy calculations to test this hypothesis would be of some interest.

Appendix

Using the defect forces defined in Fig. 4 of this paper, the strain energy E can be obtained as follows:

$$E = E_S - E_R$$

where we denote the strain energy of ions and the relaxation energy due to the interaction between forces as E_S and E_R respectively (*5–7*). In calculating E_S and E_R, we have applied linear elasticity theory to an isotropic continuum as in our previous reports (*3–7*).

In an infinite ordered array, the forces in Fig. 4 repeat periodically, so we can calculate E_S and E_R using the Fourier transformed force $\tilde{F}(\mathbf{q})$ and elastic Green's function $\tilde{G}(\mathbf{q})$. The relaxation energy is, then, written as follows (*5*):

$$E_R = (1/N)\sum_{\mathbf{r}}\sum_{\alpha} F_\alpha(\mathbf{r}) \sum_{\mathbf{q}}\sum_{\beta} e^{-i\mathbf{qr}} G_{\alpha\beta}(\mathbf{q})\tilde{F}_\beta(\mathbf{q}) \quad \text{(A1)}$$

where N is the number of the unit cells, $F_\alpha(\mathbf{r})$ represents the αth component of the defect force at $\mathbf{r}$, $\tilde{F}_\beta(\mathbf{q})$ is the βth component of the Fourier transformed force, $\tilde{G}_{\alpha\beta}(\mathbf{q})$ denotes the $\alpha\beta$th component of the Fourier transformed Green's function, $\sum_\alpha$ indicates the summation of every component of the defect force at $\mathbf{r}$ and $\sum_{\mathbf{r}}$ means the summa-

tion of the relaxation energies of all ions in the cell.

On the other hand, the strain energy of ions in the cell is assumed to be expressed by (*3–7*):

$$E_S = \sum_{\mathbf{r}} (4\pi r_{\mathbf{r}})^3 / w(\mathbf{r}) \qquad \text{(A2)}$$

where $\sum_{\mathbf{r}}$ indicates a similar meaning to that in Eq. (A1), $w(\mathbf{r})$ represents the strain energy density at $\mathbf{r}$ and $r_{\mathbf{r}}$ means the ionic radius of an ion at $\mathbf{r}$. The strain energy density for a cubic elastic continuum has the form (*12*),

$$w = \tfrac{1}{2}C_{11}\sum_{i=1}^{3} e_{ii}^2 + C_{12}\sum_{i,j=1}^{3} e_{ii}e_{jj} + 2C_{44}\sum_{i,j=1}^{3} e_{ij}^2 \qquad |i \neq j| \quad \text{(A3)}$$

where the klth component of the strain at $\mathbf{r}$, $e_{kl}(\mathbf{r})$ is given as the following (*7*):

$$e_{kl}(\mathbf{r}) = -(i/2N)\sum_{\mathbf{q}} e_{\mathbf{qr}}^{-i} \sum_{\beta} [q_l \tilde{G}_{k\beta}(\mathbf{q}) + q_k \tilde{G}_{l\beta}(\mathbf{q})]\tilde{F}_{\beta}(\mathbf{q}) \qquad \text{(A4)}$$

where every notation in Eq. (A4) has the same meaning as in Eq. (A1).

The Fourier transformed Green's function is given in Ref. (*13*) for a cubic elastic continuum as:

$$C_{44}\tilde{G}_{ij}(\mathbf{q}) = \frac{1}{q^2}\left(\Lambda_i\delta_{ij} - \Lambda_i\Lambda_j \frac{\gamma K_i K_j}{1 + \gamma \sum_{l=1,3} \Lambda_l K_l^2}\right) \qquad \text{(A5)}$$

where the K_i are the direction cosines (q_i/q) of $\mathbf{q}$ and

$$\Lambda_i(\mathbf{q}) = (1 + \delta K_i^2)^{-1}. \qquad \text{(A6)}$$

The dimensionless factors depend only on the elastic constants, C_{ij}

$$\gamma = (C_{12} + C_{44})/C_{44}$$
$$\gamma = (C_{11} - C_{12} - 2C_{44})/C_{44}. \qquad \text{(A7)}$$

The defect forces repeat under the translation $\mathbf{T}$ and all transforms $\tilde{F}(\mathbf{q})$ vanish unless $\mathbf{q}$ reflect this transformation. Then each component of wave vector $\mathbf{q}$ can be written as

$$q = (q_x, q_y, q_z)$$
$$q_x = (2\pi/a)M$$
$$q_y = (2\pi/a)P$$
$$q_z = [10\pi/a(5n - 1)]L \qquad \text{(A8)}$$

where M, P, and L are integers.

The strain energy of ions and the relaxation energy can be obtained as a sum over discrete values of q in the first Brilloin Zone of the lattice, i.e., $-(2\pi/a) < q_x$, $q_y \leqq (2/a)$ and $-(10\pi/a) < q_z \leqq (10\pi/a)$.

The defect forces and sites at which they operate are

site $\mathbf{r}$	Force $F(\mathbf{r})$
(0, 0, 2/5)	(0, 0, F)
(0, 0, −2/5)	(0, 0, $-F$)

Then each component of the Fourier transformed force $\tilde{F}(\mathbf{q})$ is written as:

$$\tilde{F}_1(\mathbf{q}) = \tilde{F}_2(\mathbf{q}) = 0$$
$$\tilde{F}_3(\mathbf{q}) = \sum_{\mathbf{r}} F(\mathbf{r}) e_{\mathbf{qr}}^{i} \qquad \text{(A9)}$$

where $\sum_{\mathbf{r}}$ t indicates the summation over sites described above.

In calculating the strain energy and the relaxation energy, we have employed the same ratio of the elastic constants as in previous papers (*3–6*) and the following ionic radii for O^{2-}, W^{4+}, and Sn^{2+} ions (*14*):

$$C_{11} : C_{12} : C_{44} = 16 : 7 : 5$$
$$r_O = 0.140 \text{ nm}$$
$$r_W = 0.060 \text{ nm}$$
$$r_{Sn} = 0.122 \text{ nm}.$$

Acknowledgments

E.I. is indebted to Professor R. Wade for his encouragement during this work, and R.J.D.T. to the Science Research Council for an equipment grant.

References

1. R. J. D. TILLEY, *Chem. Scripta* **14,** 147 (1979).
2. J. S. ANDERSON, *in* "The Chemistry of Extended Defects in Nonmetallic Solids" (L. Eyring and M. O'Keeffe, Eds.), p. 14. North-Holland, Amsterdam (1970).
3. E. IGUCHI AND R. J. D. TILLEY, *Phil. Trans. Roy. Soc. London* **A286,** 55 (1977).
4. E. IGUCHI AND R. J. D. TILLEY, *J. Solid State Chem.* **24,** 121, 131 (1978).
5. E. IGUCHI AND R. J. D. TILLEY, *J. Solid State Chem.* **29,** 435 (1979).
6. E. IGUCHI AND R. J. D. TILLEY, *J. Solid State Chem.*, **32,** 221 (1980).
7. Y. SHIMIZU AND E. IGUCHI, *Phys. Rev.* **17,** 2505 (1978).
8. R. STEADMAN, R. J. D. TILLEY, AND I. J. MCCOLM, *J. Solid State Chem.* **4,** 199 (1972).
9. T. EKSTRÖM, M. PARMENTIER, AND R. J. D. TILLEY, *J. Solid State Chem.*, **37,** 24 (1981).
10. S. IIJIMA, *J. Solid State Chem.* **14,** 52 (1975).
11. T. EKSTRÖM AND R. J. D. TILLEY, *J. Solid State Chem.* **24,** 209 (1978).
12. J. P. HIRTH AND J. LOTHE, "Theory of Dislocations," p. 29. McGraw-Hill, New York (1968).
13. P. H. DEDERICHS AND G. LEIFRIED, *Phys. Rev.* **188,** 1175 (1969).
14. R. D. SHANNON AND R. J. PREWITT, *Acta Crystallogr.* **B25,** 925 (1973).
15. A. M. STONEHAM AND P. J. DURHAM, *J. Phys. Chem. Solids* **34,** 2127 (1973).
16. E. IGUCHI AND R. J. D. TILLEY, *J. Solid State Chem.* **21,** 49 (1977).
17. R. J. D. TILLEY, *Nature (London)* **269,** 229 (1977).
18. R. JAMES AND C. R. A. CATLOW, *J. Phys.* supplement **38** (12), C7 (1977).
19. C. R. A. CATLOW AND R. JAMES, *Nature (London)* **272,** 603 (1978).
20. R. PORTIER, A. CARPY, H. FAYARD, AND J. GALY, *Phys. Stat. Sol.* (a), **30,** 683 (1975).
21. M. HERVIEN, F. STUDER, AND B. RAVEAU, *J. Solid State Chem.* **22,** 273 (1977).